RESEARCH ARTICLE

Study of Photocatalytic Nano-Particle Effects on the Low Temperature Plasma Ionization Mass Spectrometry

Dan Bee Kim,[1] Sohee Yoon[2]

[1]Center for Electriomagnetic Standards, Korea Research Institute of Standards and Science, Daejeon, 34113, Republic of Korea
[2]Center for Nano-Bio Measurement, Korea Research Institute of Standards and Science, Daejeon, 34113, Republic of Korea
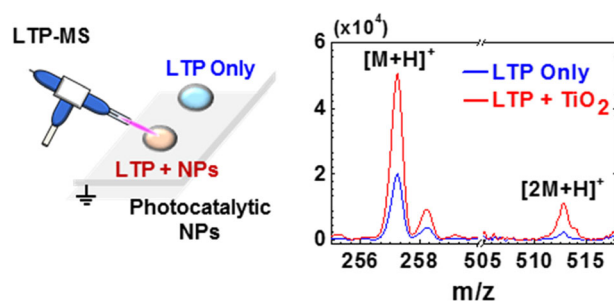
Abstract. Although the low temperature plasma mass spectrometry (LTP-MS) is widely used as an analysis tool for many biochemical samples, its application window is somehow limited to the analytes of low molecular mass and high volatility. For this reason, there have been attempts to enhance the ionization/desorption efficiencies with extra heating, for instance. In this study, another enhancement method was suggested using the photocatalytic nano-particles (NPs). In order to assess the NP effects on the LTP-MS, two fatty acid ethyl ester samples of ethyl myristate and ethyl palmitate were used, and the NP of titanium dioxide (TiO_2) was mainly employed. The results showed that the signal intensities of the LTP-MS were largely increased with the TiO_2 addition for both samples. In addition, the cholesterol sample was analyzed using the TiO_2 assisted LTP-MS, also resulting in the enhancement of the signal intensity. The overall results inferred that the photocatalytic NP confirmed its role as an effective assist tool for the LTP-MS, especially suitable because of the facile method and the heat-free nature.

Keywords: Low temperature plasma, Mass spectrometry, Photocatalytic-nanoparticles, TiO_2; Titanium dioxides

Introduction

Ambient ionization mass spectrometry (MS) is a versatile real time and direct analysis tool for the target molecules in public safety, forensics, pharmaceuticals, and agricultural fields [1–5]. MS process works in the order of sample introduction, ionization, separation of ions, and detection, and the ionization efficiency mostly decides the MS analyzing capability.

For real time and direct analysis, it is important to analyze the sample under atmospheric environment using an ambient ionization source. Various ambient ionization methods have been developed, and complex combinations of the methods have also been employed to enhance ionization efficiency: desorption electrospray ionization (DESI) [6], direct analysis in real time (DART) [7], laser ablation electrospray ionization (LAESI) [8], plasma assisted desorption ionization (PADI) [9], low temperature plasma (LTP) [10], extractive electrospray

ionization (EESI) [11], direct atmospheric pressure chemical ionization (DAPCI) [12], etc.

Among the plasma-based ambient ionization methods, LTP has some favorable features; simple and inexpensive plasma generation system and low current and temperature plasma properties as well as dry ionization process, direct sample interaction, no sample pretreatment, flexible sample type, etc. [10]. Accordingly, LTP has been actively studied and applied for biological sample analysis [13–17]. Nevertheless, the LTP has its limits analyzing target molecules with a high molecular weight and/or low volatility attributable to its soft ionization and low temperature.

Hence, there have been studies to overcome the limits by applying extra heating to the target sample in one way [18, 19]. While the heating helps the target molecules to be thermally desorbed from the sample surface, the high temperature of several hundreds °C can damage heat-sensitive biological samples. Other approaches were also studied by modifying the LTP source and by varying the sample introduction method; the LTP source was constructed with the bundle of small capillaries to allow the analysis of a large sample area, and the

detection sensitivity was significantly improved for drug molecules by direct injection of the reaction reagent into the plasma plume [20].

In this study, we have considered another assisting method using photocatalytic nanoparticles (NPs). There have been studies using the NPs as a matrix for matrix-assisted laser desorption/ionization (MALDI) in order to enhance the selectivity [21–23]. Lin et al. utilized gold nanoparticles in thermal desorption ambient mass spectrometry for analyzing small organic molecules such as amino acids, insecticides, and biodiesel samples [24]. Here, we are trying to enhance the ionization efficiency of LTP-MS with photocatalytic NPs, which are known to have synergetic effects with the plasma discharge for the destruction of chemical and biological samples [25, 26]. The synergy comes from the increment of oxygen radicals, and we assume that it will help enhance ionization efficiency without increasing sample temperature.

Titanium dioxide (TiO_2) has been proven to be the most active photocatalysis because of its photo-stability, strong oxidizing power, non-toxicity, chemical and biological inertness, etc. [27]. The UV radiation from the plasma discharge excites the TiO_2 and generates the electron and hole pairs, which are capable of initiating a series of chemical reactions [28].

Fatty acid methyl/ethyl esters are the representative target molecules in many bio-applications using MS as they play significant roles in all organisms as the structural components of the cell membranes by relaying signals from the extracellular environment to the intracellular network [29, 30]. For this reason, several studies about LTP-MS analysis have been done using fatty acid ethyl esters [19, 31–33].

In this study, we analyzed two different fatty acid ethyl esters of ethyl myristate and ethyl palmitate independently using LTP-MS, then applied the photocatalytic TiO_2 to improve the LTP ionization efficiency. We investigated the density effects for the fatty acid ethyl ester samples and TiO_2, and other types of photocatalytic NPs were compared as well. Last but not the least, cholesterol sample with a low volatility was analyzed to further confirm the enhancement effect of photocatalytic NPs on LTP-MS.

Experimental

Low Temperature Plasma

The low temperature plasma (LTP) source consists of a glass tube (O.D. 1/8 inch and I.D. 1/16 inch) with an inner pin electrode (stainless steel, O.D. 1.0 mm) as shown in Figure 1. An alternating current (AC) high voltage of 1 kV was supplied to the pin electrode at a frequency of 10 kHz. The AC voltage was provided using a power amplifier (KSC 300, Korea Switching Co., Korea) and a function generator (DG4062, RIGOL Technologies Inc., USA) of which the output voltage was the sine wave. An indium tin oxide (ITO) coated glass was placed on the sample holder and connected to the ground. The powered and grounded electrode configuration and its material type is relatively flexible since there is little effect on the LTP-

MS measurement results. Helium gas of 99.999 % purity was supplied at a flow rate of 0.6 L/min as a discharge gas. Samples were positioned at about 3 mm away from the MS inlet, and the LTP source was placed at about 3 mm away from the sample tilted with an angle of about 45 °.

Sample Preparation

All chemicals were purchased from Sigma-Aldrich Korea (Seoul, South Korea). Analyte solutions of ethyl myristate were prepared with concentration of 0.02, 0.04, 0.09, and 20 mg/mL in ethanol. Ethyl palmitate solutions were prepared in ethanol at concentrations of 2.5, 5, 10, 25 mg/mL, respectively. Cholesterol solution was prepared at 10 mg/mL in ethanol.

TiO_2 NPs of 1, 3, 10, 30 mg of were suspended in 1 mL of ethanol, respectively. For other nanoparticles, 30 mg of zinc oxide (ZnO) and aluminum dioxide (Al_2O_3) also were suspended in 1 mL of ethanol, respectively.

The sample solution containing ethyl ester and NPs was prepared by mixing each solution at a volume ratio of 1:1. Each sample solution was vortexed for about 30 seconds before loading the sample. For LTP-MS analysis, 5 μL of sample solution was loaded into the circular well chamber with 3 mm in diameter and 1 mm in depth in order to keep the size of the loaded sample constant and let dry in the air.

Before optimizing the sample preparation method, several other ways were attempted: layering the NPs and the sample, scattering the NPs on top of the sample, and using a double-sided tape for the NPs. Each attempt showed different results on the degree of enhancement in LTP-MS detection sensitivity, but the enhancement was still observed even in the worst case.

Mass Spectrometry

Mass spectrometry was performed in positive ion mode on a linear ion trap mass spectrometer (LTQ XL, Thermo Scientific, USA) and Xcalibur software 3.0 (Thermo Scientific, USA) for acquiring the data. The analyte ions or clusters containing them generated by LTP in the atmosphere were carried through a transfer MS inlet into to the vacuum interface. Mass spectrometric conditions were optimized as follows: capillary temperature, 250 °C; capillary voltage, 35 V; and tube lens voltage, 110 V; capillary voltage, 55 V; and tube lens voltage, 90 V. The mass spectra were collected with the maximum ion injection time of 100 ms and one microscan per spectrum and with the normal scanning rate of 60 μs/u. The spectra were acquired continuously for about 30 seconds over the mass to charge ratio (m/z) range from 150 to 800.

Nanoparticle Photocatalysts

Titanium dioxide (TiO_2) NP was purchased from Evonik Korea (Seoul, South Korea). The specific model used was AEROXIDE TiO_2 P25: white powder consisting of about 80%–90% anatase and the rest in rutile form. Specific surface area (BET) is 50 ± 15 m^2/g. The particles are several hundred nm in size, and the primary particle has a mean diameter of
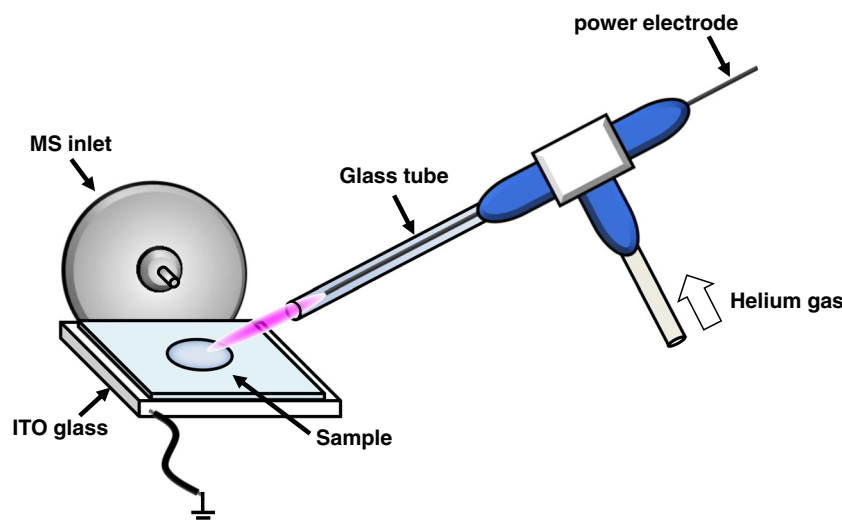
Figure 1. Schematic of the low temperature plasma ionization source placed at the inlet of the mass spectrometer with the sample holder

about 21 nm. The energy difference between the valence and the conduction bands in the solid state is 3.0 eV for rutile and 3.2 eV for anatase [34].

Zinc oxide (ZnO) NP was manufactured by BASF (Ludwigshafen, Germany). The specific model used was Z-COTE. The average particle size is less than 200 nm. The energy difference between the valence and the conduction bands is 3.37 eV [35].

Aluminum oxide (Al_2O_3) NP was purchased from Evonik Korea (Seoul, South Korea). The specific model used was AEROXIDE Al_2O_3 65: white power consisting of primary particles sized approximately 7 to 40 nm. Specific surface area (BET) is 65 m^2/g. The energy difference between the valence and the conduction bands is 3.64 eV [36].

Results and Discussions

Photocatalytic NPs were employed to improve the detection efficiency of the LTP-MS. Two representative fatty acid ethyl ester samples of ethyl myristate and ethyl palmitate were chosen as analytes for LTP-MS, and the TiO_2 was mainly used as the photocatalytic NP. The enhancement effects of the photocatalytic NPs on LTP-MS were studied by controlling various experimental parameters of the sample density, the NP density, and the NP type.

Fatty Acid ethyl Esters with TiO_2

Figure 2 illustrates the mass spectra of ethyl myristate (a) for different sample densities and (b) for with and without TiO_2 cases together with the integrated peak intensities (c) for monomer and (d) dimer ions. Each spectrum was acquired for about 30 seconds then time-averaged, because the signal intensity was almost invariant against the acquisition time. Acquisition was repeated three times for each measurement condition. The

m/z of ethyl myristate protonated molecular ion is 257.3, and its vapor pressure is 2.00×10^{-3} mmHg at 25 °C. First, under the LTP only condition of Figure 2a, the ion peak value increases from 10^4 to 10^5 with the sample density increment. With the TiO_2 added, the ion peak value increased more than two times for the same sample density of 0.02 mg/mL as shown in Figure 2b. For a more accurate comparison, the area under the ion peaks were integrated as in Figure 2c for the monomer of m/z 257.3 and Figure 2d for the dimer of m/z 513.8. The integrated intensities of the ion peaks increased as much as five times with the addition of TiO_2 compared with LTP only case.

When the ethyl myristate sample density was increased further up by 10 times to about 20 mg/mL, an interesting behavior was observed as presented in Figure 3. With the addition of TiO_2, the dimer ion peak was greatly increased from 1.4×10^6 to 9.6×10^6, becoming much higher than the monomer ion peak. While the dimer ion peak was largely increased, the monomer ion increased little from 2.0×10^6 to 2.2×10^6. The dimer ion peak was also detected under the LTP only condition but with the lower intensity compared with the monomer ion peak. A sign for such behavior was already seen under the lower sample densities. The integrated intensity increment of the monomer ion was similar as in Figure 2c, but that of the dimer ion or the slope of Figure 2d became larger for the increasing sample density.

Dimers are observed at almost double the monomer ion m/z value, and they are formed by their own associations, produced more likely under the high sample density condition as shown in Figure 2a. Esters are strong bases in the gas phase, so they are readily ionized by proton transfer. Also, the dimer ions of the esters, formed by the proton binding of the two carboxylic oxygens, are very stable [37], meaning that the probability for the proton-bound dimer formation of the ethyl myristate will be increased under the proton enriched condition. As a result of the further proton enrichment by the TiO_2 assist, the dimer ions
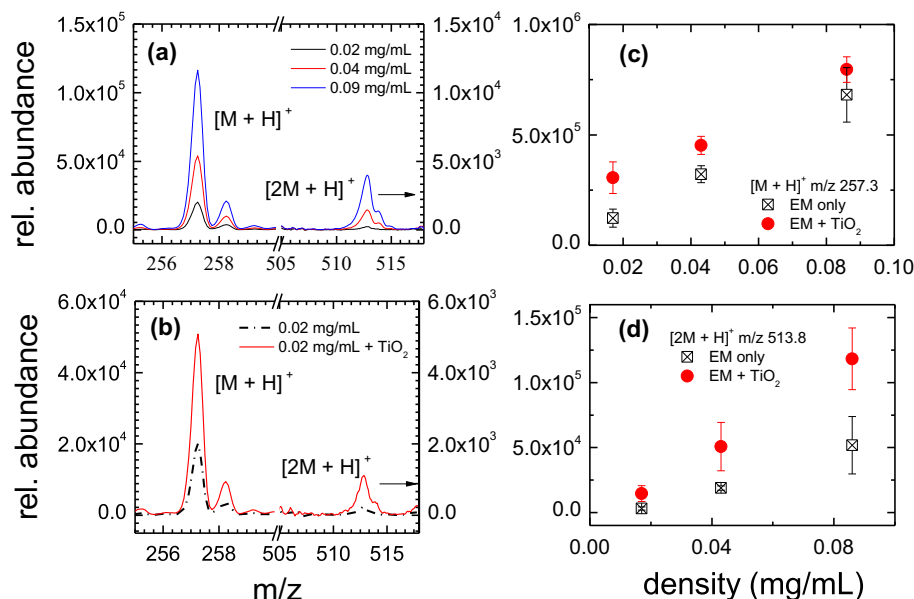
Figure 2. The mass spectra of ethyl myristate **(a)** for different sample densities, and **(b)** for with and without TiO$_2$ cases. The integrated intensities of the peaks corresponding to **(c)** the monomer and **(d)** the dimer ions

are more likely to be produced as Figure 3. In other words, the dramatic increase of the ethyl myristate dimer under the high sample concentration condition is attributed to the high production of the protons with the interaction between the plasma discharge and the TiO$_2$.

Figure 4 shows the mass spectra of ethyl palmitate (a) for different sample densities and (b) for with and without TiO$_2$ cases together with the detected peak area (c) for monomer. The ethyl palmitate has the *m/z* 285.3 and the vapor pressure of 7.00×10^{-5} mmHg at 25 °C. First, under the LTP only condition of Figure 4a, the ion peak value increased with sample density increment. With the addition of the TiO$_2$, the ion peak value increased from 6.5×10^3 to 1.6×10^4, which is more than two times for the same sample density of 25 mg/mL as shown

in Figure 4b. The areas under the ion peaks were obtained as in Figure 4c for the monomer of *m/z* 285.3, and the enhancement can be seen with the addition of the TiO$_2$ compared with the LTP only case. It is noted that the ion peaks of ethyl palmitate are one or two orders less in their intensities when compared with the ethyl myristate even at the higher sample densities. The lower ion peak intensities can be explained with the vapor pressure difference. Ethyl palmitate has a lower vapor pressure by about two orders than the ethyl myristate, and the low vapor pressure means that the samples are less volatile and remain intact on the slide glass, being difficult to be desorbed from the surface. Hence, the ethyl palmitate with the lower vapor pressure resulted the lower detection efficiency for the LTP-MS and so did its dimer ions as shown insets of Figure 4a and b.

The target molecular ion is detected through the hydrogen ion (or proton) attachment. There are water molecules in the ambient, and the most abundant background ions in the plasma-based ambient desorption/ionization sources are protonated water clusters (H$_2$O)$_n$H$^+$ [28]. Thus, LTP becomes a good ionization source for MS, and the number of positive hydrogen atoms and oxygen radicals increases even more according to the below reactions when TiO$_2$ is introduced: the electron-hole pair is produced with UV irradiation, and the production of OH radical and H$^+$ is followed [38].

$$TiO_2 + h\nu \rightarrow TiO_2(e^- + h^+) \tag{1}$$
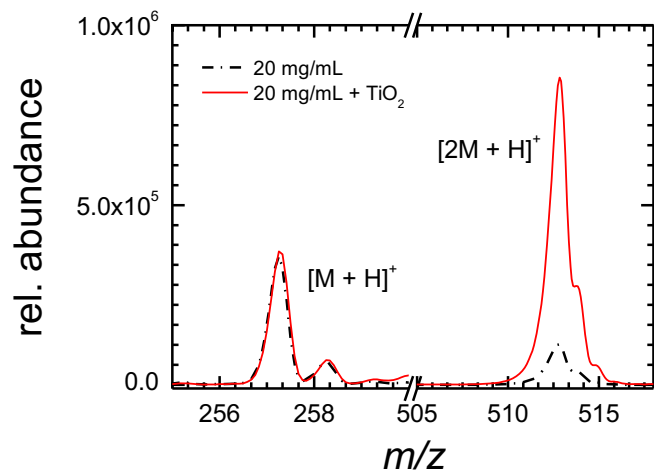
$$H_2O + h^+ \rightarrow {}^*OH + H^+ \tag{2}$$

Figure 3. The mass spectra of ethyl myristate at a high sample density of 20 mg/mL for with and without TiO$_2$ cases

In the previous study [26], the increment of the oxygen radicals including *OH was observed indirectly from the plasma light emission spectrum. Also, it was found that the plasma

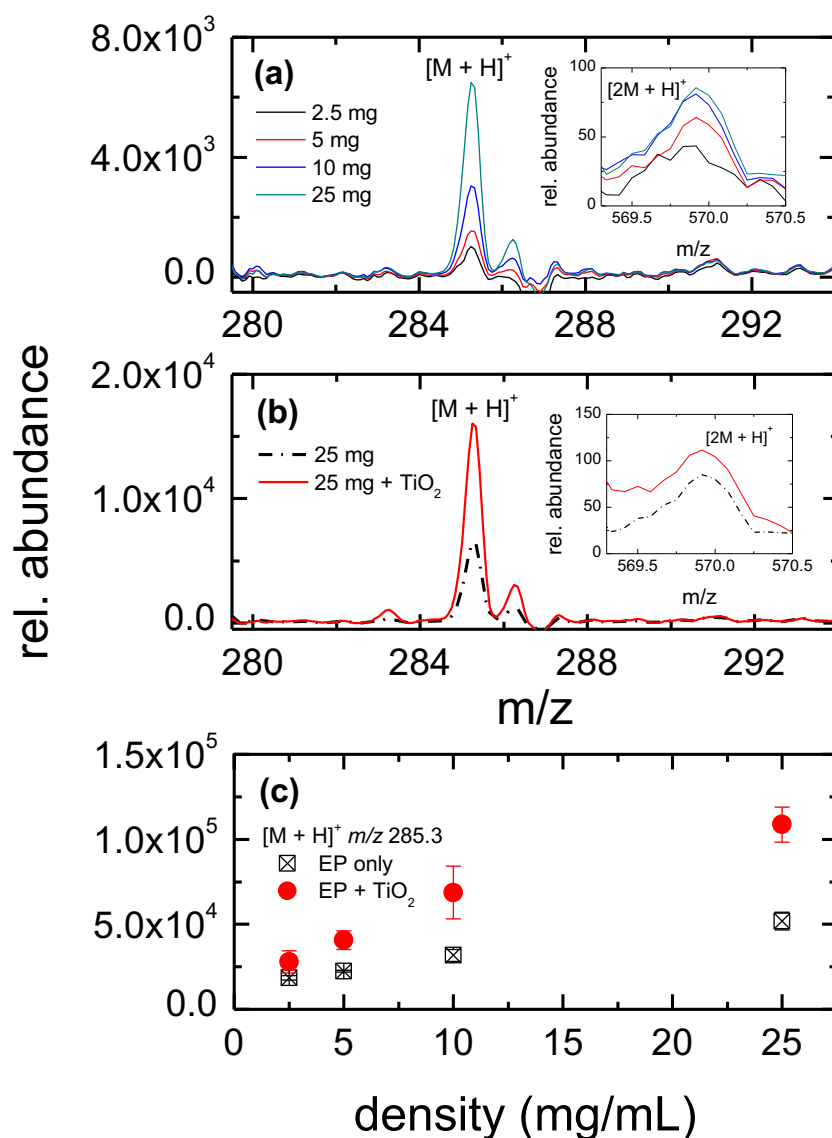**Figure 4.** The mass spectra of ethyl palmitate **(a)** for different sample densities and **(b)** for with and without TiO_2 cases. **(c)** The integrated intensity of the monomer ion peak

induces defect energy levels in the TiO_2, leading to the easier generation of oxygen radicals by lowering the UV absorbance energy to the visible range. Moreover, the average electron energy increases or more electrons are in the high energy tail in the plasma with the TiO_2 [39]. Summing up, the interaction between the plasma discharge and the TiO_2 makes the resulting plasma a stronger ionization tool for the LTP-MS. For such reasons, it was clearly seen from the fatty acid ethyl ester samples of ethyl myristate and ethyl palmitate that their signal intensities detected by LTP-MS were greatly enhanced with the TiO_2. The TiO_2 assist method is attractive in many ways since it is easy, inexpensive, and most of all safe and heat-free.

Nanoparticle Density and Types

The effect of the TiO_2 density was studied using ethyl myristate; density was fixed at either 0.04 mg/mL or 0.09 mg/mL. The integrated intensities of the monomer and dimer ion peaks are presented in Figure 5 for varying TiO_2 density from 0 (none) to 30 mg/mL. For both of the monomer and dimer ion peaks, the integrated intensities increased rapidly from 0 to 1 or 3 mg/mL, then saturated for the higher densities of the TiO_2. The high density TiO_2 can hinder the photocatalysis by making the effective surface area of NP smaller because of the aggregation [40].

There are several photocatalytic NPs other than TiO_2, and others of ZnO and Al_2O_3 were used for comparison. As can be seen Figure 6, all the photocatalytic NPs enhanced the detection efficiency of the LTP-MS for the ethyl myristate detection, and TiO_2 was the most effective amongst all. The integrated intensities of the monomer ion peak was 2.9×10^5 for the LTP only case, then increased to 1.1×10^6 for TiO_2, 6.4×10^5 for ZnO, and 6.1×10^5 for Al_2O_3, respectively.
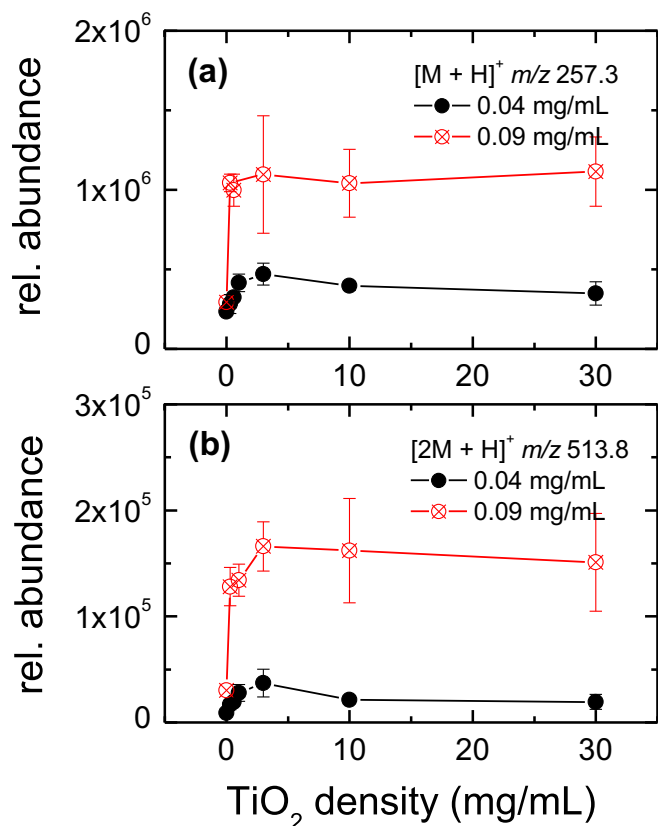
Figure 5. The integrated intensities of the peaks corresponding to **(a)** the monomer and **(b)** the dimer ions for the ethyl myristate with TiO₂ density varying from 0 (none) to 30 mg/mL

The band gap energies of the NPs do not differ much as mentioned before, but when listed in the ascending order it is as follows: TiO_2, ZnO, Al_2O_3. The TiO_2 has the lowest band gap energy amongst them, and the band gap energy order matches the ionization enhancement order. Yet, the different behaviors of the NPs, especially the TiO_2, seem to come from their interaction with the plasma discharge. Under sunlight, ZnO is known to be more active than TiO_2 with more light absorption
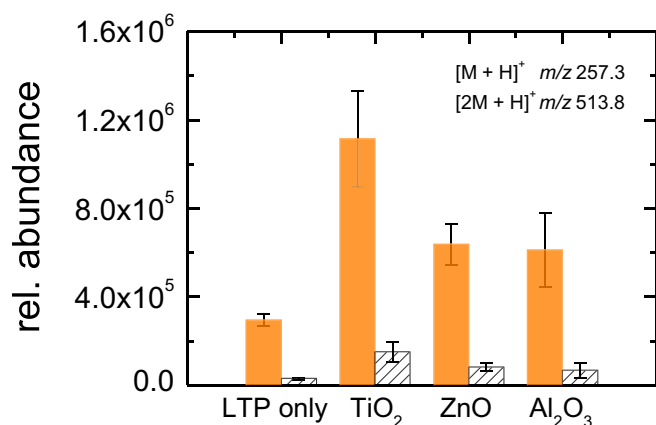

Figure 6. The integrated intensities of the monomer and dimer ion peaks of the ethyl myristate for different types of photocatalytic NPs
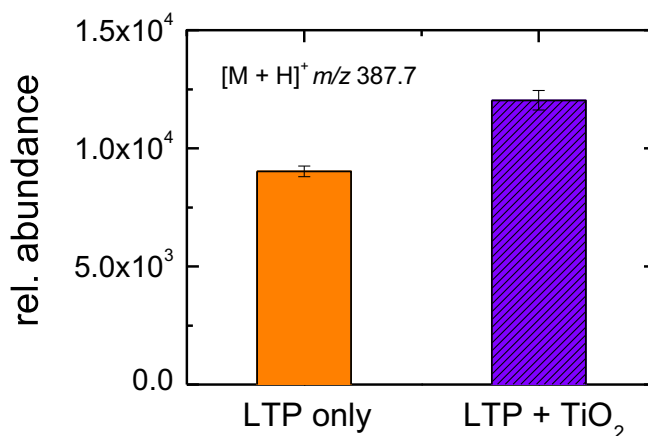

Figure 7. The integrated intensities of the monomer ion peak for the cholesterol under with and without TiO_2 conditions

in the visible region [40]. However, under plasma, TiO_2 becomes more absorbent to visible light as defect energy levels are produced because of oxygen vacancies [26, 41]. As a result, the band gap energy of the TiO_2 is decreased by plasma discharge, so the electron-hole pairs are more likely to be abundant, leading to the more efficient ionization source for the analyte.

Cholesterol

After studying the effects of photocatalytic NPs on LTP-MS using the fatty acid ethyl esters samples, the cholesterol sample was used to further investigate the TiO_2 assist. Cholesterol is a sterol, a type of lipid molecule, an essential structural component of all animal cell membranes, and it also serves as a precursor for the biosynthesis of steroid hormones related to diseases such as Alzheimer's [42]. For such reasons, cholesterol analysis is significant and garners much interest. However, it is difficult to generate a gas-phase ion for the cholesterol because of the low proton affinity and acidity [43]. Besides, the m/z of cholesterol molecular ion is 387.7, and its vapor pressure is 7.8×10^{-10} mmHg at 25 ℃; rather high molecular weight and low volatility. Hence, additional treatment is needed for the LTP-MS analysis of the cholesterol to enhance the ionization efficiency (or yield).

Figure 7 illustrates the integrated intensities of cholesterol monomer ion peaks for LTP only and with TiO_2 cases. The integrated intensities are relatively smaller than the fatty acid ethyl ester samples as expected, but with the aid of the TiO_2, the intensity increased from 9.0×10^3 to 1.2×10^4. At the same time, the peak height almost doubled. It is important to note that photocatalytic NPs can be applied to improve the LTP-MS detection sensitivity for the analytes of high molecular weight and low volatility.

Conclusions

In order to improve LTP-MS detection efficiency, an enhancement method using photocatalytic NPs was suggested and studied with two fatty acid ethyl ester samples of ethyl

myristate and ethyl palmitate. For the photocatalytic NPs, TiO_2 was mainly employed. The measurement results showed that LTP-MS together with the NPs greatly increased the signal intensities for both samples. In the case of ethyl myristate, the signal intensity increased as much as five times with TiO_2 assist compared with LTP alone. The degree of enhancement varied (increased) against the TiO_2 density, but it was saturated for TiO_2 density of 3 mg/mL and above. Additionally, several types of photocatalytic NPs were compared; TiO_2 was the most effective compared with ZnO and Al_2O_3. Last but not the least, cholesterol of very low volatility was analyzed using LTP-MS for with and without the TiO_2, and the signal intensity also increased with the addition of TiO_2. The overall results inferred that the use of photocatalytic NPs effectively enhances the detection efficiency of the LTP-MS in a quite easy way and most importantly without any thermal stresses on the heat-sensitive bio-samples.

In this study, the samples were prepared by mixing with the NPs in ethanol solution. For real application to biological tissues, it can be difficult to apply such a mixing method. Under such circumstances, another method of spraying the NPs on the sample surface can be more appropriate. Also, the sample density should be much lower for real bio-sample analysis. Hence, follow-up studies will be conducted based on this study, regarding the optimization of the photocatalytic NP assist methods for the real biological samples, which will naturally involve maximization of measurement sensitivity and/or extension of detection mass limit.

Acknowledgements

References

1. Weston, D.J.: Ambient ionization mass spectrometry: current understanding of mechanistic theory; analytical performance and application areas. Analyst. **135**, 661–668 (2010)
2. Garcia-Reyes, J.F., Harper, J.D., Salazar, G.A., Charipar, N.A., Ouyang, Z., Cooks, R.G.: Detection of explosives and related compounds by low-temperature plasma ambient ionization mass spectrometry. Anal. Chem. **83**, 1084–1092 (2011)
3. Takats, Z., Wiseman, J.M., Cooks, R.G.: Ambient mass spectrometry using desorption electrospray ionization (DESI): instrumentation, mechanisms, and applications in forensics, chemistry, and biology. J. Mass Spectrom. **40**, 1261–1275 (2005)
4. Lawton, Z.E., Traub, A., Fatigante, W.L., Mancias, J., O'Leary, A.E., Hall, S.E., Wieland, J.R., Oberacher, H., Gizzi, M.C., Mulligan, C.C.: Analytical validation of portable mass spectrometer featuring interchargeable, ambient ionization sources for high throughput forensic evidence screening. J. Am. Soc. Mass Spectrom. **28**, 1048–1059 (2017)
5. Wiley, J.S., Garcia-Reyes, J.F., Harper, J.D., Charipar, N.A., Ouyang, Z., Cooks, R.G.: Screening of agrochemicals in foodstuffs using low-temperature plasma (LTP) ambient ionization mass spectrometry. Analyst. **135**, 971–979 (2010)
6. Takats, Z., Wiseman, J.M., Gologan, B., Cooks, R.G.: Mass spectrometry sampling under ambient conditions with desorption electrospray ionization. Science. **306**, 471–473 (2004)
7. Dane, A.J., Cody, R.B.: Selective ionization of melamine in powdered milk by using argon direct analysis in real time (DART) mass spectrometry. Analyst. **135**, 696–699 (2010)
8. Nemes, P., Vertes, A.: Laser ablation electrospray ionization for atmospheric pressure, in vivo, and imaging mass spectrometry. Anal. Chem. **79**, 8098–8106 (2007)
9. Ratcliffe, L.V., Rutten, F.J.M., Barrett, D.A., Whitemore, T., Seymour, D., Greenwood, C., Aranda-Gonzalvo, Y., Robinson, S., McCoustra, M.: Surface analysis under ambient conditions using plasma-assisted desorption/ionization mass spectrometry. Anal. Chem. **79**, 6094–6101 (2007)
10. Harper, J.D., Charipar, N.A., Mulligan, C.C., Zhang, X.R., Cooks, R.G., Ouyang, Z.: Low-temperature plasma probe for ambient desorption ionization. Anal. Chem. **80**, 9097–9104 (2008)
11. Chen, H.W., Venter, A., Cooks, R.G.: Extractive electrospray ionization for direct analysis of undiluted urine, milk and other complex mixtures without sample preparation. Chem. Commun. **11**, 2042–2044 (2006)
12. Takats, Z., Cotte-Rodriguez, I., Talaty, N. Chen, H. Cooks, R.G.: Direct, trace level detection of explosives on ambient surfaces by desorption electrospray ionization mass spectrometry. Chem. Commun. **15**, 1950–1952 (2005)
13. Kong, M.G., Kroesen, G., Morfill, G., Nosenko, T., Shimizu, T., Van Dijk, J., Zimmermann, J.L.: Plasma medicine: an introductory review. New J. Phys. **11**, 115012 (2009)
14. Graves, D.B.: The emerging role of reactive oxygen and nitrogen species in redox biology and some implications for plasma applications to medicine and biology. J. Phys. D. Appl. Phys. **45**, 263001 (2012)
15. Gweon, B., Kim, H., Kim, K., Kim, M., Shim, E., Kim, S., Choe, W., Shin, J.H.: Suppression of angiogenesis by atmospheric pressure plasma in human aortic endothelial cells. Appl. Phys. Lett. **104**, 133701 (2014)
16. Ali, A., Kim, Y.H., Lee, J.Y., Lee, S., Uhm, H.S., Cho, G., Park, B.J., Choi, E.H.: Inactivation of propionibacterium acnes and its biofilm by non-thermal plasma. Curr. Appl. Phys. **14**, S142–S148 (2014)
17. Gong, S., Shi, S., Gamez, G.: Real-time quantitative analysis of valpronic acid in exhaled breath by low temperature plasma ionization mass spectrometry. J. Am. Soc. Mass Spectrom. **28**, 678–687 (2017)
18. Huang, G., Ouyang, Z., Cooks, R.G.: High-throughput trace melamine analysis in complex mixtures. Chem. Commun. **45**, 556–558 (2009)
19. Lee, H.J., Oh, J.S., Heo, S.W., Moon, J.H., Kim, J.H., Park, S.G., Park, B.C., Kweon, G.R., Yim, Y.H.: Peltier heating-assisted low temperature plasma ionization for ambient mass spectrometry. Mass Spectrom. Lett. **6**, 71–74 (2015)
20. Dalgleish, J.K., Wleklinski, M., Shelley, J.T., Mulligan, C.C., Quyang, Z., Cooks, R.G.: Arrays of low-temperature plasma probes for ambient ionization mass spectrometry. Rapid Commun. Mass Spectrom. **27**, 135–142 (2013)
21. Wen, X., Dagan, S., Wysocki, V.H.: Small-molecule analysis with silicon-nanoparticle-assisted laser desorption/ionization mass spectrometry. Anal. Chem. **79**, 434–444 (2007)
22. Chen, C., Chen, Y.: Molecularly imprinted TiO_2-matrix-assisted laser desorption/ionization mass spectrometry for selectively detecting r-cyclodextrin. Anal. Chem. **76**, 1453–1457 (2004)
23. Wang, M.-T., Liu, M.-H., Wang, C.R.C., Chang, S.Y.: Silver-coated gold nanoparticles as concentrating probes and matrices for surface-assisted laser desorption/ionization mass spectrometric analysis of aminoglycosides. J. Am. Soc. Mass Spectrom. **20**, 1925–1932 (2009)
24. Lin, J.-Y., Chen, T.-Y., Chen, J.-Y., Chen, Y.-C.: Multilayer gold nanoparticle-assisted thermal desorption ambient mass spectrometry for the analysis of small organics. Analyst. **135**, 2668–2675 (2010)
25. Harling, A.M., Demidyuk, V., Fischer, S.J., Whitehead, J.C.: Plasma-catalysis destruction of aromatics for environmental clean-up: Effect of temperature and configuration. Appl. Catal. B Environ. **82**, 180–189 (2008)

26. Jung, H., Kim, D.B., Gweon, B., Moon, S.Y., Choe, W.: Enhanced inactivation of bacterial spores by atmospheric pressure plasma with catalyst TiO$_2$. Appl. Catal. B Environ. **93**, 212–216 (2010)

27. Xiaohong, W., Xianbo, D., Wei, Q., Weidong, H., Zhaohua, J.: Enhanced photo-catalytic activity of TiO$_2$ films with doped La prepared by micro-plasma oxidation method. J. Hazard. Mater. B. **137**, 192–197 (2006)

28. Chan, G.C.Y., Shelley, J.T., Wiley, J.S., Engelhard, C., Jackson, A.U., Cooks, R.G., Hieftje, G.M.: Elucidation of reaction mechanisms responsible for afterglow and reagent-ion formation in the low-temperature plasma probe ambient ionization source. Anal. Chem. **83**, 3675–3686 (2011)

29. Spector, A.A., Yorek, A.: Membrane lipid composition and cellular function. J. Lipid Res. **26**, 1015–1035 (1985)

30. Graber, R., Sumida, C., Nunez, E.A.: Fatty acids and cell signal transduction. J. Lipid Mediat. Cell Signal. **9**, 91–116 (1994)

31. Zhang, J.I., Costa, A.B., Tao, W.A., Cooks, R.G.: Direct detection of fatty acid ethyl esters using low temperature plasma (LTP) ambient ionization mass spectrometry for rapid bacterial differentiation. Analyst. **136**, 3091–3097 (2011)

32. Kim, S.H., Jang, H.J., Park, J.H., Lee, H.J., Kim, J., Yim, Y.-H., Kim, D.B., Yoon, S.: Comparison of desorption enhancement methods in the low temperature plasma ionization mass spectrometry for detecting fatty acids in *Drosophila*. Curr. Appl. Phys. **17**, 1120–1126 (2017)

33. Zhang, J.I., Tao, W.A., Cooks, R.G.: Facile determination of double bond position in unsaturated fatty acids and esters by low temperature plasma ionization mass spectrometry. Anal. Chem. **83**, 4738–4744 (2011)

34. Pfeifer, V., Erhart, P., Li, S., Rachut, K., Morasch, J., Brötz, J., Reckers, P., Mayer, T., Rühle, S., Zaban, A., Seró, I.M., Bisquert, J., Jaegermann, W., Klein, A.: Energy band alignment between anatase and rutile TiO$_2$. J. Phys. Chem. Lett. **4**, 4182 (2013)

35. Kumar, D.D., Nair, P.B., Justinvictor, V.B., Thomas, P.V.: Structural and optical properties of zinc oxide nanorods prepared by aqueous solution route. Chemist. **89**, 1 (2016)

36. Filatova, E.O., Konashuk, A.S.: Interpretation of the changing the band gap of Al$_2$O$_3$ depending on its crystalline form: connection with different local symmetries. J. Phys. Chem. C. **119**, 20755–20761 (2015)

37. Marotta, E., Paradisi, C.: Positive ion chemistry of esters of carboxylic acids in air plasma at atmospheric pressure. J. Mass Spectrom. **40**, 1583–1589 (2005)

38. Ghezzar, M.R., Abdelmalek, F., Belhadj, M., Benderdouche, N., Addou, A.: Enhancement of the bleaching and degradation of textile wastewaters by Gliding arc discharge plasma in the presence of TiO$_2$ catalyst. J. Hazard. Mater. **164**, 1266–1274 (2009)

39. Tu, X., Gallon, H.J., Whitehead, J.C.: Electrical and spectroscopic diagnostics of a single-stage plasma-catalysis system: Effect of packing with TiO$_2$. J. Phys. D. Appl. Phys. **44**, 482003 (2011)

40. Sakthivela, S., Neppolianb, B., Shankarb, M.V., Arabindoob, B., Palanichamyb, M., Murugesanb, V.: Solar photocatalytic degradation of azo dye: comparison of photocatalytic efficiency of ZnO and TiO$_2$. Sol. Energy Mater. Sol. Cells. **77**, 65–82 (2003)

41. Rehman, S., Ullah, R., Butt, A.M., Gohar, N.D.: Strategies of making TiO$_2$ and ZnO visible light active. J. Hazard. Mater. **170**, 560–569 (2009)

42. Puglielli, L., Tanzi, R.E., Kovacs, D.M.: Alzheimer's disease: the cholesterol connection. Nat. Neurosci. **6**, 345–351 (2003)

43. Wu, C., Ifa, D.R., Manicke, N.E., Cooks, R.G.: Rapid, direct analysis of cholesterol by charge labeling in reactive desorption electrospray ionization. Anal. Chem. **81**, 7618–7624 (2009)